A Role for ELOVL4 in the Mouse Meibomian Gland and Sebocyte Cell Biology

Anne McMahon,[1] Hua Lu,[1] and Igor A. Butovich[1,2]

[1]Department of Ophthalmology, University of Texas Southwestern Medical Center, Dallas, Texas, United States
[2]Graduate School of Biomedical Sciences, University of Texas Southwestern Medical Center, Dallas, Texas, United States

Correspondence: Igor A. Butovich, Department of Ophthalmology, University of Texas Southwestern Medical Center, 5323 Harry Hines Boulevard, Dallas, TX 75390-9057, USA;
igor.butovich@utsouthwestern.edu.

Submitted: September 25, 2013
Accepted: March 17, 2014

Citation: McMahon A, Lu H, Butovich IA. A role for ELOVL4 in the mouse meibomian gland and sebocyte cell biology. *Invest Ophthalmol Vis Sci.* 2014;55:2832–2840.DOI:10.1167/iovs.13-13335

Purpose. The meibum lipidome contains lipids with extremely long chain fatty acid (ELCFA) residues, longer than C_{28}. Particular lipids based on extremely long chain (*O*-acyl)-ω-hydroxy fatty acids (OAHFA) are found in all mammal meibum and are proposed to stabilize the tear film by forming the interphase between its lipid and aqueous sublayers. The enzyme ELOVL4 is required for synthesis of ELCFA. We investigated whether Stgd3 mice, harboring mutations in ELOVL4 that have been shown to decrease the levels of its biosynthetic lipid products, would represent a model system in which to define the role of such lipids in meibum.

Methods. Ocular phenotypes of wild-type mice were compared with those of Stgd3 mice. ELOVL4 expression in eyelid and back skin was characterized by immunohistochemical analysis. Anatomical changes within the eyelids of mutant mice were examined by hematoxylin and eosin staining of paraffin-embedded tissue.

Results. Mutant mice had increased eyelid blink rates, a reluctance to maintain their eyes fully open, protruding meibomian gland (MG) orifices, and anatomical changes within the MG. In wild-type mice, ELOVL4 was strongly expressed within the holocrine meibomian and sebaceous glands. The enzyme localized to structures encircling lipid deposits within cells in both the early and late stages of differentiation. No ELOVL4 was detected within the central meibomian duct.

Conclusions. Stgd3 mice show changes that resemble clinical findings in patients with the evaporative type of dry eye disease, suggesting that further studies in this mouse model will provide a basis for better understanding of the causes of human dry eye.

Keywords: ELOVL4, lipids, meibocytes, sebocytes, tear film

Meibomian glands (MG) are located within the tarsal plate in both the upper and the lower eyelids of humans and in a wide variety of other animal species.[1,2] These glands synthesize a very complex mixture of lipids[3–6] that are delivered to the outer surface of the eye where they form the outermost layer of the multilayered tear film (TF), called the tear film lipid layer (TFLL).[4,7] A properly functional TF and, importantly, its TFLL are critical for ocular health, contributing to both a functional barrier against desiccation and maintenance of a clear interface between the external environment and the corneal surface. Considerable effort has been devoted both in early studies[6,8,9] and in more recent ones, with use of more sophisticated methodology by multiple investigators,[5,10–12] to defining the qualitative and quantitative lipid composition of human and animal meibum. In addition, there is a general consensus that alterations in MG function and/ or alteration in the qualitative/ quantitative composition of the lipids secreted by the MG are significant contributors to the evaporative form of dry eye dysfunction (DED [or disease]), a usually chronic condition that effects millions of people each year.[2,13]

The majority of meibum lipids (~70%) are nonpolar in nature, composed predominantly of cholesteryl ester (CE) and wax ester (WE) lipids, which form the bulk phase of the TFLL. In addition, meibum contains amphiphilic lipids such as fatty acids (FA) and (*O*-acyl)-ω-hydroxy FA (OAHFA), which represent ~5% of meibum lipids, and their (chole)steryl esters.[4,12,14] An unusual chemical signature of all of the OAHFA-based lipids, and some of the other nonpolar lipids such as CE, is their content of extremely long chain fatty acid (ELCFA), with residues $>C_{28}$. In mammals, the synthesis of FA with $>C_{16}$ requires an endoplasmic reticulum (ER)-localized fatty acid elongation system. The rate-limiting condensation step in this system is catalyzed by 1 of the 7 enzymes of the elongase of long chain fatty acid family (ELOVL1–ELOVL7), each member of which demonstrates its own substrate specificity. The only ELOVL that has been shown to have activity in in vitro studies[15–17] toward substrates $>C_{26}$ in length is ELOVL4, thus suggesting a role for ELOVL4 in elaborating components of the meibum lipidome.

The *ELOVL4* gene was initially identified as a consequence of studies establishing that multiple different mutations in the human gene are linked to autosomal dominant Stargardt disease 3 (STGD3 descriptor 600110; Online Mendelian Inheritance in Man [OMIM]).[18–21] Subsequently, multiple *Elovl4* mutant mouse models were generated to investigate the biological basis of STGD3. These included both knockout[22,23] and knockin models carrying introduced disease-associated mutations mapping to the C terminus of ELOVL4.[24–26] All C-terminal mutations cause loss of the peptide sequence required to target the enzyme to the ER.[27] Studies in mutant mice established a vital requirement for the lipid biosynthetic products of ELOVL4 for viability. All homozygous *Elovl4* mutant mice died as

neonates as a consequence of disruption of the barrier function of the skin.[23–26,28] Lipid analysis studies in the skin and retina of heterozygous *Elovl4* mutants documented a reduction of approximately 50% of complex lipid species containing C_{28} or longer FA as one component and the absence of such lipids in homozygous mutants. Specific affected lipids in the retina were phosphatidylcholines with polyunsaturated C_{28} to C_{34} acyl residues[29] and, in the skin, multiple lipids including acylceramides that contained monounsaturated C_{28} to C_{36} acyl residues with ω-hydroxyl groups.[24–26] Thus, studies to date in *Elovl4* mutant mice suggest that (1) ELOVL4 is required for synthesis of diverse lipid species containing very long chain FA $>C_{28}$; (2) synthesis of such lipids occurs endogenously in the tissues where they are found; and (3) loss of the unique lipid biosynthetic products of ELOVL4 can have significant biological consequences within the tissues where they are synthesized.

In this article we report robust expression of ELOVL4 in mouse MG and present data to suggest that mice carrying mutations in *Elovl4* present with ocular characteristics suggestive of the evaporative form of DED. We further propose that *Elovl4* mutant mice represent a unique model system which can be studied to delineate the role of specific classes of meibomian lipids in ocular TF function.

Methods

Mice

All procedures involving mice were approved by the University of Texas Southwestern Medical Center (UTSW) Institutional Animal Care and Use Committee and were conducted in accordance with the Association for Research in Vision and Ophthalmology Statement for the use of Animals in Ophthalmic and Vision Research. Animals were housed at UTSW in facilities which have been certified by the Association for Assessment and Accreditation of Laboratory Animal Care International (AAALAC). Both wild-type (WT) and heterozygous *Elovl4* mutant mice (heterozygous Stgd3 mice) were used in this study, the latter strain was generated as a knockin model of human STGD3.[26] Both the WT and heterozygous Stgd3 mice were maintained on a mixed, predominantly 129SvEv and C57BL6 background.

Immunohistochemistry

Eyelid tissue, including both the epidermis and MG with attached conjunctiva, the eyeball, and midline back skin were dissected from animals after euthanasia and fixed overnight at 4°C in freshly prepared 4% paraformaldehyde in PBS, pH 7.4. Samples were cryopreserved by passage through 10%, 20%, and 30% sucrose in PBS before mounting in optimal cutting temperature compound (OCT; Tissue-Tek, Torrance, CA, USA). Tissues were sectioned and placed on Superfrost Plus slides (Thermo Scientific; Fisher Scientific, Pittsburgh, PA, USA) and stored at −20°C. Sections for immunostaining were air dried for 30 minutes, washed with PBS to remove OCT, and permeabilized and blocked by incubation for 20 minutes in PBS containing 0.1% Triton X-100 in the presence of 10% (vol/vol) normal goat serum. A rabbit affinity-purified anti-mouse ELOVL4 antibody, kindly provided by Gene Anderson MD, PhD (Oklahoma Medical Center),[15] diluted 1:200, was incubated with tissue overnight at 4°C in PBS containing 2.5% normal goat serum. After incubation, samples were washed 3 times for 5 minutes with PBS and incubated for 1 hour with Alexa Fluor 488-conjugated F(ab)2 fragment of a goat anti-rabbit secondary (1:500 dilution; Molecular Probes, Life Technologies, Grand Island, NY, USA). After being washed 3 times for 5 minutes with PBS, nuclei were counterstained by incubation with 4′,6-diamidino-2-phenylindole (DAPI; SelectFX nuclear labeling kit; Molecular Probes) for 2 minutes, washed with PBS, and mounted in Gel/Mount (Biomeda Corp, Foster City, CA, USA). Stained sections were examined using a DM1300B fluorescent microscope (Leica Microsystems, Inc., Buffalo Grove, IL, USA) with fluorescein isothiocyanate (excitation at 470/40 nm, and emission at 525/50 nm) and ultraviolet (excitation at 360/40 nm, and emission at 470/40 nm) filters and equipped with a CoolSNAP fx digital camera (Photometrics, Tucson, AZ, USA). Images were acquired individually using each filter set and later processed using Photoshop (Adobe Systems, Inc., San Jose, CA, USA) to combine the signals in the final red-green-blue images.

Oil Red O Staining

Oil Red O (ORO) staining solution was prepared as described previously.[5] Cryosections of eyelid and skin were used for ORO staining protocols because this method preserves tissue lipid during processing. To stain, sections that had been permeabilized, blocked, and incubated with both primary and secondary antibodies, as described earlier, were washed 3 times for 5 minutes with PBS and then incubated for 30 minutes with a working dilution of ORO that had been filtered through a 0.2-μm filter immediately before use. Sections were then washed for 30 minutes with water and mounted directly, using Gel/Mount, or nuclei were counterstained with DAPI and then mounted. ORO staining was examined by fluorescent microscopy using a Texas red filter (excitation at 560/40 nm, emission at 645/75 nm).

Hematoxylin and Eosin Staining

Eyelids were removed, fixed for at least 24 hours in buffered Carson's formalin,[30] and then dehydrated by successive passage through 50%, 70%, 95%, and 100% ethanol before paraffin embedding. Tissue was sectioned, rehydrated through decreasing ethanol concentrations, and stained with hematoxylin and eosin (H&E; Statlab Medical Products, McKinney, TX, USA).

In Situ Hybridization

Anesthetized adult WT mice were perfused with freshly prepared 4% paraformaldehyde in PBS prepared with diethylpyrocarbonate-treated water. Dorsal skin was removed and fixed in the same solution overnight at 4°C. The tissue was paraffin embedded, sectioned, and processed for hybridization in the Molecular Biology Core Laboratory at UTSW, using established procedures.[31] Probes used to detect *Elovl4* mRNA were 291 nucleotide sense and antisense sequences corresponding to nucleotides 546 to 836 from mouse Elovl4 cDNA sequence (NCBI designation NM_148941). Probes were transcribed using T7 RNA polymerase in the presence of ^{35}S-labeled uridine-5′-triphosphate. Following autoradiography and development, slides were counterstained with hematoxylin, dehydrated, and cover-slipped with permanent mounting medium.

Results

Mice Carrying Mutations in Elovl4 Show Changes in Eyelid Phenotype

Observation of mice at weaning in our breeding colony of Stgd3 mice revealed the presence of animals with 2 different

Investigative Ophthalmology & Visual Science

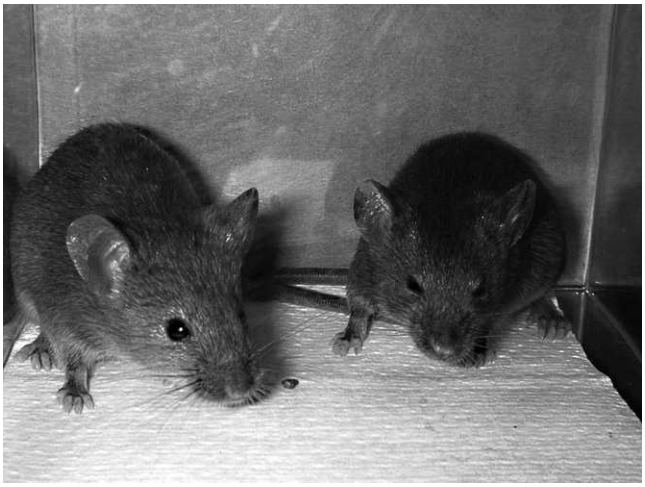

FIGURE 1. Gross eye phenotypes in WT and heterozygous Stgd3 mice. The eyes of a 1-month-old WT mouse (*left*) are rounded in appearance, whereas those in a heterozygous Stgd3 littermate mouse (*right*) present with an elongated profile.

gross eye phenotypes. Some mice displayed a round, open eye profile, whereas others presented a more slanted eye phenotype (Fig. 1). Genotyping of pups for the presence of the *Elovl4* and *Stgd3* alleles revealed that the round eye profile was found in WT mice, whereas the altered profile tracked with the presence of a single *Stgd3* allele. Although homozygous Stgd3/Stgd3 animals were also born in the colony from heterozygous Stgd3 pairings, such animals died within hours of birth as a consequence of epidermal barrier defects.[26] Thus, such animals were not available for monitoring effects on gross open eye phenotypes because eye development in mice is completed in the postnatal period.

Both male and female heterozygous Stgd3 mice showed the altered eye phenotype, but some interanimal variability in the degree of the slanted eye appearance was observed. With experience in the mouse room, it became possible for us to genotype mice at weaning based on gross eye phenotypes. Closer observation of individual 1- to 2-month-old heterozygous Stgd3 mice revealed that the slant eye phenotype reflected a pattern where these mice chose to keep their eyes only partially opened when at rest. Such mice when startled, however, were capable of opening their eyes more completely. By partially closing their eyes, the heterozygous Stgd3 mice reduced the effective area of exposed cornea. To obtain an estimate of the extent of reduction in exposure, we recorded movies for 2 sets of littermates: WT and heterozygous Stgd3 mice, freely moving in a confined space. Individual frames in which mice were shown at rest were isolated and the pixel count of the exposed corneal surface was determined for each animal, using Photoshop. This analysis showed a reduction in the exposed corneal surface area in heterozygous Stgd3 mice of 46% to 50% compared to that of WT mice.

Analysis of the movie recordings of mice further revealed that heterozygous Stgd3 mice displayed an increase blink rate relative to that observed in WT mice. Quantitative measurement of blink rates in freely moving mice is challenging because of their speed and agility and also the small size of their eyes. However, our analysis of movies recorded for mice of both genotypes revealed that WT mice blink infrequently. Observation of most WT mice over a 2-minute period showed no blinking or, infrequently, a maximum of 1 blink. This contrasted with heterozygous Stgd3 mice, where multiple blinks, up to a maximum of 6 in some animals, were observed.

Genotype-associated difference were also noted in the appearance of the everted eyelid margins of mice. Aligned along the margins of both the upper and lower eyelids are the orifices from the central ducts of the MG, located in the tarsal plates. These orifices were either poorly visible or were identified only as very small areas lacking pigmentation in the eyelid margins of 1- to 2-month-old male and female WT mice when examined with a dissecting microscope (Fig. 2A). This is in marked contrast to the observed profile of MG orifices in heterozygous Stgd3 mice. While evenly spaced along both the upper and lower eyelids, the orifices in heterozygous Stgd3 mice presented as raised white domes protruding above the surface of the eyelid margin (Fig. 2B). Indeed, such was the extent of protrusion that all orifices were clearly visible even without the aid of a microscope. The meibum material had a white, toothpaste-like appearance and could be readily expressed from the protruding domes with application of very mild pressure on either side of the eyelid. In WT mice, in contrast, less meibum was available for expression, and it was either more liquid or had a colorless toothpaste-like appearance. Although the MG orifices were clearly visible in 1- to 2-month old heterozygous Stgd3 mice, there was no noticeable swelling of their eyelids relative to WT mice, nor was there any readily observable evidence of excess tear production.

Expression of Elovl4 in Meibomian Glands

Immunofluorescent staining of WT mouse eyelid with a rabbit polyclonal anti-mouse ELOVL4 antibody revealed intense ELOVL4 staining in the MG (Fig. 3A). This same pattern of staining was also observed in heterozygous Stgd3 mice. In the MG, ELOVL4 staining was present in regions aligned along all sides of the central meibomian ducts (Fig. 3A, see the duct marked by the asterisk), as they extended through the length of the tarsal plate. The stained regions are the MG acini where the lipid-synthesizing meibocyte cells reside. In contrast, no ELOVL4 staining was observed within the lipid mass in the central duct regions. In addition to the MG staining, the antibody also stained the outer layers of the keratinized skin epidermis (Fig. 3A). Staining of retinal sections in the same experiment showed the expected strong ELOVL4 staining in

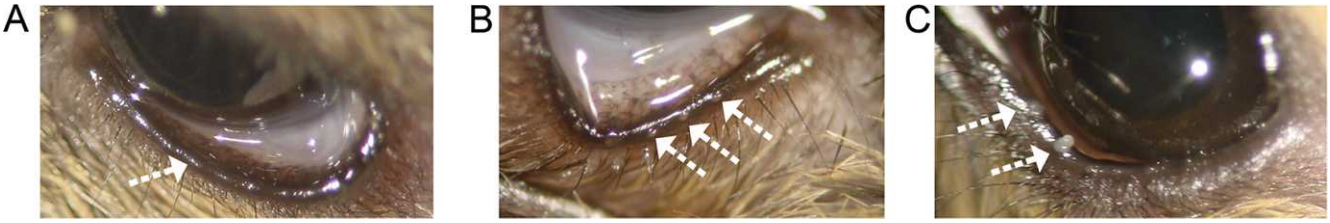

FIGURE 2. MG orifices on the eyelid margin. (**A**) In the everted eyelid of a WT mouse, the MG orifices are poorly visible (*arrow*). (**B**) In heterozygous Stdgd3 eyelids, meibum within the central MG duct forms a dome which protrudes above the MG orifices (*multiple arrows*). (**C**) Expression of meibum from a heterozygous Stgd3 mouse eyelid at room temperature elicits secretion of white toothpaste-like secretions (*arrows*).

Investigative Ophthalmology & Visual Science

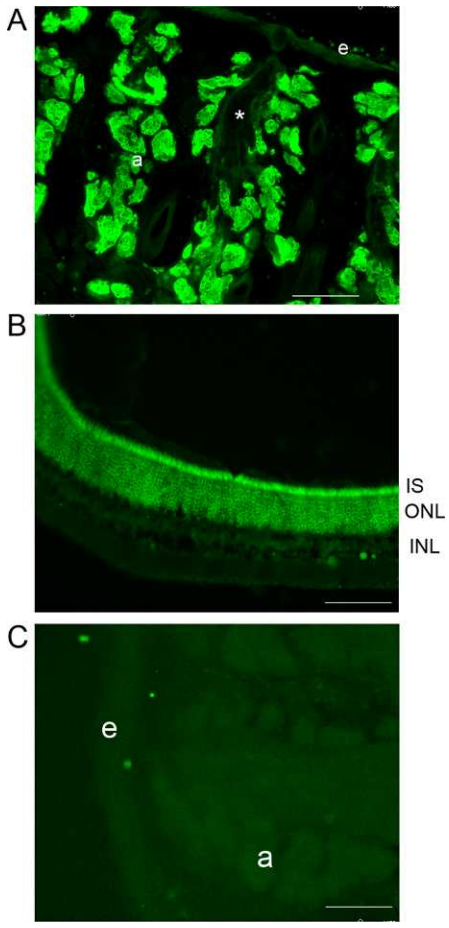

Figure 3. Expression of *ELOVL4* in mouse eyelid. (**A**) Strong ELOVL4 immunolabeling (*green*) was present in the MG, with labeling at a much lower intensity in the outer layers of the epidermis (**e**). Labeling within the MG was observed in the acini (**a**) lining the central duct but not within the duct itself (*asterisk*). (**B**) In mouse retina, the same ELOVL4 antibody showed the expected pattern of strong labeling in photoreceptor inner segments (IS) and in their cell bodies in the outer nuclear layer (ONL). (**C**) In the absence of the primary anti-ELOVL4 antibody, no staining was observed in eyelid tissue. *Scale bars*: 100 μm.

photoreceptor cell bodies in the outer nuclear layer and in the inner segments of the same cells (Fig. 3B). Labeling, at a much lower intensity, and thus poorly visible in Figure 3B, was also detected in the lower layers of the retina, consistent with previous reports of low levels of Elovl4 there.[15] When the ELOVL4 primary antibody was omitted during staining of the mouse eyelid, no labeling was observed in either the MG or the epidermis (Fig. 3C).

The MG is a holocrine gland, and both lipid synthesis and release of the lipid products occur within the acini. ORO staining of the eyelid showed 2 types of lipid deposits within the MG. Bulk lipid deposits were observed within the central duct region of the gland (Fig. 4A), whereas more discrete lipid droplets were present within cells in the acini regions (Fig. 4B). Within MG, acini meibocytes undergo a pattern of differentiation, starting from proliferating basal undifferentiated cells in the periphery and progressing to intermediate nucleated cells, which, as a consequence of lipid synthesis, contain cellular lipid droplets.[32] The acini examined at higher magnification showed the presence of nucleated cells on the periphery with a decrease in the number of nuclei, as detected by DAPI staining, toward the center. Neither ELOVL4 nor ORO staining was found associated with the peripheral layer of cells (Fig. 4B). However, staining for both was detected in all cells, progressing through the differentiation process within the acini.

ORO staining showed the presence of very small spherical structures, likely lipid droplets, within cells initiating differentiation and immediately abutting the undifferentiated periphery cells (Fig. 4B). As meibocytes were displaced toward the center of the acini, the ORO-stained droplets increased in size and appeared more irregular in shape. In all meibocytes where ORO-stained droplets were detected, strong ELOVL4 staining was observed and in no case was an overlap observed between ELOVL4 and ORO staining. The cellular ELOVL4 staining showed a distinctive fenestrated pattern which surrounded all ORO-positive structures, including both the small droplets in the more peripheral cells and the larger droplets seen in more fully differentiated cells (Fig. 4). With the exclusion of the ORO-positive and nuclear DAPI-stained structures, the ELOVL4-positive structures were spread throughout the remaining cellular spaces. This extensive expression of ELOVL4 and its location in close proximity to the sites of accumulation of lipids within the meibocytes supports an important role for this enzyme in the elaboration of the MG lipidome.

Expression of ELOVL4 in Sebocytes

Examination of the pattern of ELOVL4 staining in mouse eyelids revealed that in addition to the epidermis and MG, the enzyme was also expressed in other structures (Fig. 4A). Some of these were located on either side of hair follicles present on the epidermal side of the eyelid. This location suggests such structures were likely sebaceous glands. Like the MG, sebaceous glands are holocrine glands containing cells (sebocytes) that secrete a very complex mixture of lipids into the hair follicle and from there to the skin surface. Previous studies in both mouse and humans have documented within this mixture lipids containing ELCFA $>C_{26}$.[33,34] The presence of such lipids would suggest a role for ELOVL4 in sebum synthesis within sebocytes. Consistent with such a role, in-situ hybridization analysis detected expression of *Elovl4* mRNA in sebocytes located in mouse back skin with an anti-sense *Elovl4* riboprobe but no signal with use of a sense probe (Fig. 5A). The observed sebaceous gland pattern of grain deposition is similar to that previously reported for another member of the ELOVL enzyme family, ELOVL3.[35] Immunohistochemical analysis of mouse back skin showed a very strong staining for ELOVL4 in skin sebocytes and a much weaker staining for the protein in the suprabasal layers of the epidermis (Fig. 5B). In the sebaceous glands, as in the MG, the cellular ELOVL4 staining pattern was extensive, fenestrated in appearance, and encircled ORO-stained lipid droplets of different sizes. Nucleated cells lacking either ORO or ELOVL4 staining were also observed, and these likely represented undifferentiated sebocytes (Fig. 5C).

Eyelid Changes in Heterozygous Stgd3 Mice

To investigate whether structural and/or functional changes underlie the observed phenotypic changes, the eyelids of WT and heterozygous Stgd3 mice were processed and stained with H&E. In mice of both genotypes, the central meibomian duct and the meibocyte containing acini aligned around it were clearly visible (Fig. 6). The staining suggested the presence of a more enlarged or "open" space in the central duct region in heterozygous Stgd3 mice relative to that observed in WT mice (compare Figs. 6A, 6B). In addition, more intraductal debris was consistently observed in the central duct region in heterozygous Stgd3 mice (Fig. 6C, asterisk). During normal

Investigative Ophthalmology & Visual Science

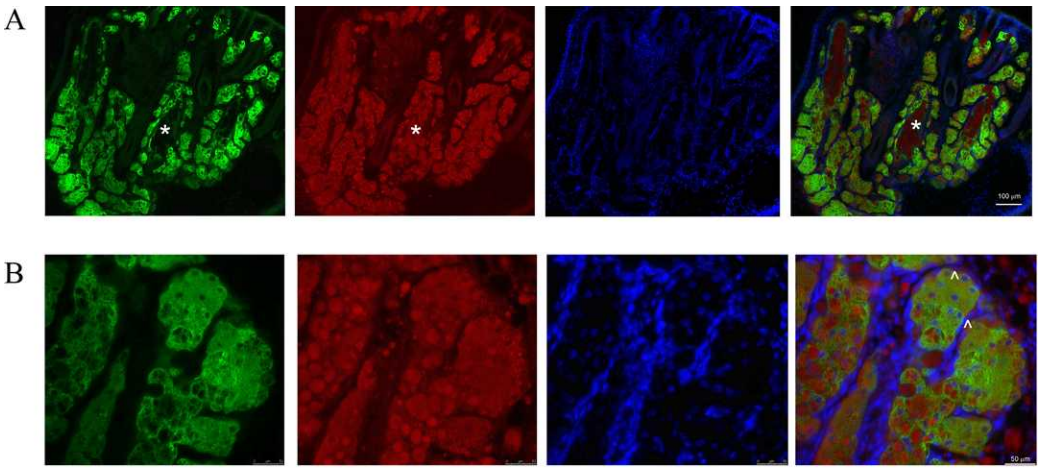

Figure 4. ELOVL4 expression and lipid deposits in mouse eyelid. Elovl4 (*green*), lipid (stained with ORO [*red*]), and nuclear (DAPI [*blue*]) staining of the upper eyelid of a 1-month-old WT mouse. (**A**) ELOVL4 and ORO staining showed no overlap in the eyelid. ORO-stained spherical lipid deposits within the MG acini and bulk amorphous lipid deposits (*) within the central MG duct are shown. Note the absence of ELOVL4 staining in the central duct region. (**B**) In the MG acini, the nuclei of the basal layer of undifferentiated meibocytes were visible, but these cells did not appear to express ELOVL4 (*arrowheads*). As meibocytes differentiated toward the center of the acini, the number of nucleated cells decreased, and the size of the lipid droplets increased. ELOVL4 staining surrounded both the small distinct ORO-stained droplets in cells closest to the basal layer and the large blob-like ORO-stained structures present toward the center of the acini.

meibocyte differentiation within acini, cells rupture and release their lipid cargo into the ductile space, and most cellular remnants are then "lost" before the lipid is delivered to the central duct. In heterozygous Stgd3 eyelids, H&E staining showed that abundant cellular membrane remnants remained within ductiles even as they were located close to where they emptied into the central duct space (Fig. 6).

In addition to changes in the MG, changes were also noted in the conjunctiva in mutant mice. Clearly visible within the conjunctiva of H&E-stained eyelid sections were prominent cells with noticeable blue cytoplasmic staining, which were most likely mucin-secreting goblet cells (Figs. 6E, 6F). In WT conjunctiva these cells occurred predominantly as single cells, the density of which varied depending on where the

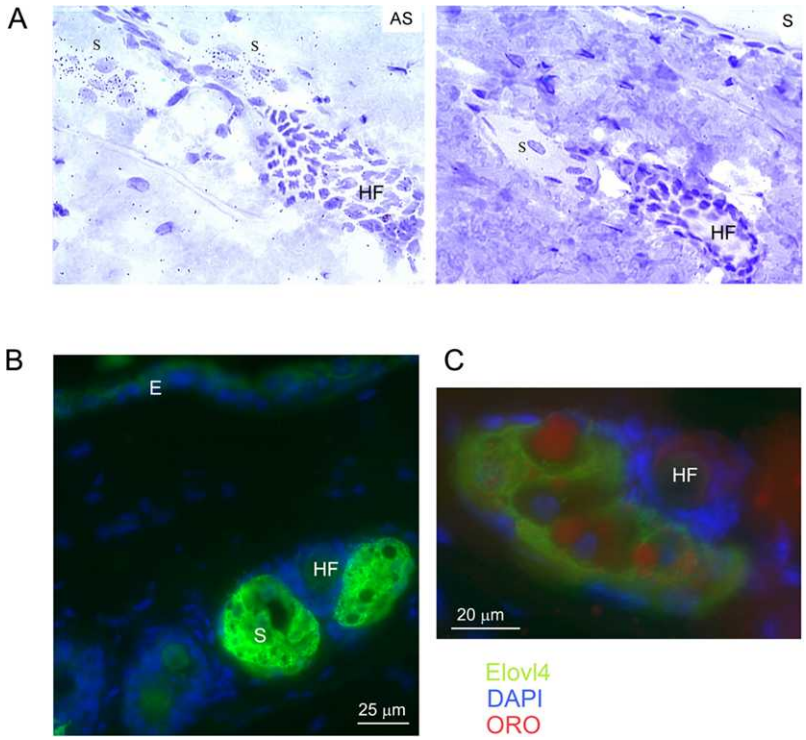

Figure 5. Expression of ELOVL4 in sebocytes in the back skin of WT mice. (**A**) In situ hybridization analysis detected abundant expression of *Elovl4* mRNA in skin sebocytes as shown by the significant presence of silver grains over sebocytes (S) in tissue hybridized with an antisense (AS) and not with a sense (S) *Elovl4* probe. Note also the absence of signal in the hair follicle (HF). (**B**) Immunohistochemical analysis further showed expression of ELOVL4 (*green*) in both the sebocytes (S) and in the epidermis (E). Nuclei were stained with DAPI (*blue*). (**C**) In skin sebocytes, ELOVL4 staining surrounded but did not overlap with lipid deposits stained with ORO (*red*).

Investigative Ophthalmology & Visual Science

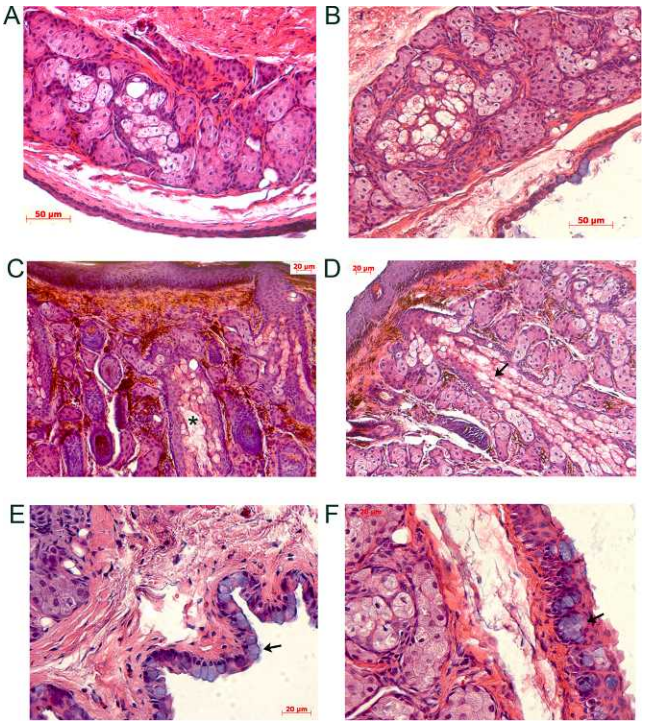

Figure 6. Eyelid alterations in heterozygous Stgd3 mice as revealed by H&E staining. Staining of meibomian glands within the TP in the upper eyelids of 3-month-old WT (**A**) and heterozygous (**B**, **C**, **D**) Stgd3 mice. The ductal space where meibum resides prior to secretion is seen in all MG images, but this area appeared enlarged in images from different sectioning planes in all mutant eyelids (**B**, **C**, **D**). In mutant animals, abundant cellular debris was evident in the central duct (**C**, *asterisk*), and extensive disintegrating cellular ruminants were prominent in acini ductiles as they merged toward the central duct (**D**, *arrow*). Within the conjunctiva of the eyelid, goblet cells, with their prominent *blue-stained* cytoplasm (*arrows*), were present as individual cells in WT eyelids (**E**) and as clusters in heterozygous Stgd3 eyelids (**F**).

conjunctiva was examined. Goblets cells are normally present at higher densities toward the nasal part of the conjunctiva. In heterozygous Stgd3 conjunctiva, goblet cells predominantly formed clusters as opposed to being present as individual cells (Fig. 6F). In addition, examination of stained sections from many WT and heterozygous Stgd3 mice suggested an increased number of goblets cells in the eyelids of heterozygous Stgd3 mice relative to that seen in WT mice.

Discussion

The MG are responsible for synthesis of the bulk of the lipid components of the TFLL, and these lipids are delivered to the ocular surface as meibum is secreted through the meibomian ducts with each blink. In this study, we showed that mice carrying a heterozygous inactivating mutation in *Elovl4* present with a gross eye phenotype wherein they are observed at rest to maintain their eyelids in a position that minimizes exposure of the ocular surface to the environment. In addition, histological studies showed both robust expression of ELOVL4 in the MG and alterations in the eyelids of mutant mice, consistent with a role for ELOVL4 and its lipid biosynthetic products in MG physiology.

Progress has been made toward delineating the chemical nature of the hundreds of different lipid species present in the meibum of humans and other species.[5,11,12] However, little progress has been made in defining either how such a complex mixture of lipids is elaborated in the MG or what the specific roles of the multitude of different lipid species are. In meibum from mammals, the most abundant classes of lipids are the nonpolar WE and CE, which together may account for more than 70% of meibum lipids.[4,5] A characteristic feature of the meibomian lipidome is a very high content of very long chain, C_{16} to C_{34} FA (some of which are present as free FA[36]) and fatty alcohol FAL residues. Although most FA in CE varies from C_{24} to C_{27}, a small fraction of the esterified FA is longer.[14,37] Within WE lipids, the carbon chain lengths of the FA have been shown to range from approximately C_{15} to C_{20},[38] whereas the FAL ranged from C_{18} to C_{32} and possibly longer.[10] In addition, meibum from all species contains significant levels (approximately 5%) of extremely long chain OAHFA and also their cholesteryl esters.[4,12,14] In both human and mouse, the ω-hydroxylated FA residues are monounsaturated and range in length from C_{28} to C_{34}.[5]

In mammals, the synthesis of FA $>C_{16}$, where not available from the diet, requires the ER-localized FA elongation system. The initial condensation and rate-limiting reaction of this system is catalyzed by 1 of 7 ELOVL.[39,40] Each elongase catalyzes substrate-specific elongation of FA of different lengths and degrees of unsaturation. Published studies have shown that some *ELOVL* genes are expressed ubiquitously (*ELOVL1*, *ELOVL5*, and *ELOVL6*), whereas the remainder show more restricted patters of expression.[40] Among the latter is the *ELOVL4* gene, which initially came to prominence as a consequence of studies establishing that multiple different mutations in the human gene are linked to autosomal dominant Stargardt disease 3.[18–21] In addition, this gene was also shown to be expressed in the skin, testes, and brain.[15,16,41] Subsequent in vitro studies suggested that the enzyme was unique in that it is the only elongase to elongate all FA with chains longer than C_{28}.[15–17] The lipid products of ELOVL4, which in a tissue-specific manner, can be saturated, monounsaturated, or polyunsaturated, have to date been detected only in tissues that express the gene.

Robust expression of ELOVL4 was observed in mouse MG, consistent with the presence in meibum of significant quantities of lipids containing ELCFA. The ocular phenotypes observed in mice carrying a single *Stgd3* allele, a mutation which causes loss of enzyme activity, points to critical roles for ELOVL4 lipid products. Such products in WT mice are most abundant in OAHFA and WE lipids.[5] The OAHFA lipids, as a consequence of their unique chemical structures and properties, have been proposed to be the amphiphilic lipids that form the critical interphase between the aqueous sublayers of the TF and the nonpolar meibum lipids that form the evaporative barrier.[7,10] Recently this hypothesis gained experimental support from in vitro studies using a chemically synthesized analog of meibomian OAHFA.[42] It is plausible that reduction in the levels of the amphiphilic lipids would destabilize the TF lipid layer, hamper its spreading, cause faster than normal evaporation of the aqueous component of the TF, and its eventual collapse. Also, ELOVL4 products with $>C_{28}$ are found in the nonpolar fraction of TF lipids, such as cholesteryl esters of OAHFA, WE, and CE.[5,14] Thus, a decline in their ratio relative to other lipid species may impact the properties of the nonpolar bulk of the TF lipid layer, too. Specifically, a decline in very and extremely long chain lipids may affect the melting characteristics of meibum by lowering its melting temperature, thus changing its delicate liquid-crystal structure.[43,44]

In addition to the changes observed in the MG of mutant mice, histological analysis also suggested changes in conjunctival Golgi cells. These cells are distributed throughout the palpebral and bulbar conjunctiva and in the fornix in a species specific pattern, with nonuniform distributions reported in individual animals in these regions.[45] Golgi cells in palpebral

Investigative Ophthalmology & Visual Science

conjunctiva in heterozygous Stgd3 mice were frequently observed in cell clusters in contrast to the single cells more frequently observed in WT mice. In mice these cells synthesize and secrete the soluble mucins Muc5ac and Muc5b. The secreted mucins are proposed to have roles in removal of debris from the surface of the eye and act as surfactants allowing spread of the TF over the ocular surface.[46] A similar phenotypic change in Golgi cells has also been reported in *Muc5ac* knockout mice,[47] where in response to loss of Muc5ac, an increase in the expression of Muc5b was observed. Our immunohistochemical studies did not reveal any expression of ELOVL4 in cells within the mouse conjunctiva. Thus, Golgi cell changes in heterozygous Stgd3 mice likely reflect a compensatory response to ocular surface changes. Although loss of Golgi cells has been reported in patients with chronic DED,[48] the relationship between ocular mucin levels and development of DED may be different. A recent study in postmenopausal women with moderate to severe disease showed up-regulation of ocular membrane mucins and a trend for increases in cellular MUC5AC in patients with mild to moderate DED.[49] The early changes observed in the Golgi cells of Stgd3 mice suggests that future studies in these mice may provide insights into the relationships among TF lipids, mucins, and ocular surface health.

In the MG ELOVL4, expression was detected throughout the acini surrounding the central meibomian ducts, with no expression seen within the lipid-enriched contents of the central duct. The presence of ELOVL4 in all meibocytes, with the exception of the basal undifferentiated cells at the periphery of the acini, is consistent with observations from previous ultrastructural studies in mouse and human MG.[32,50] The peripheral undifferentiated cells were characterized by their abundant mitochondria and low content of ER membranes and a paucity of lipid droplets. As meibocytes proceeded through holocrine differentiation, increasing amounts of smooth ER membrane were observed, and cells increased in size as a consequence of accumulating lipid products. The ER membranes were observed in close proximity to and encircled spherical structures that were proposed to contain the cellular deposits of lipids.[32,50,51] Consistent with its ER localization, ELOVL4 immunolabeling was observed to encircle both the small ORO-stained lipid droplets seen in meibocytes as they initiated differentiation, as well as in the larger ORO-stained droplets located in more differentiated cells toward the center of the acini. This pattern suggests that synthesis of lipids containing ELCFA residues is initiated in situ very early in the meibocyte differentiation process and continues throughout differentiation. However, what is currently unknown is how and where in the biosynthetic pathways the FA chains are elongated in relation to other reactions that occur to derive complex lipids such as OAHFA, sterol containing OAHFA, and FAL with very long chain residues ($>C_{26}$).

In addition to establishing the presence of and a role for ELOVL4 in the MG, our studies also point to a role for the C_{26} enzyme in synthesis of the sebum lipidome. This is the first time (to our knowledge) that sebaceous gland expression of ELOVL4 has been reported. Sebocytes, like MG, are holocrine glands and secrete a complex mixture of lipids that contributes to the barrier function of the skin and to host defense.[52] Early lipid analyses of human sebum identified within hydrolyzed lipid extracts the presence of FA residues $>C_{26}$ in length,[34] suggestive of a requirement for ELOVL4 elongation activity. While this early study was unable to assign these FA to a specific lipid class, a more recent characterization of human sebum lipids by tandem mass spectrometry analyses showed that such FA are components of the large free FA pool present in sebum.[33] In sebocytes present in the back skin of mice, as in the MG, ELOVL4 staining was found in close proximity to sites of accumulation of lipid deposits as identified by ORO staining. As in the MG, nucleated cells devoid of ORO-stained droplets showed no ELOVL4 staining. In more mature sebocytes, the staining encircled both smaller and larger lipid droplets, suggesting an ongoing requirement for ELCFA synthesis during sebocytes maturation.

In this study we showed that ELOVL4 is expressed at significant levels within the MG in the tarsal plates of mouse eyelids. Previous characterization of the lipidome of mouse meibum has documented that it has a lipid profile more similar to human meibum than the profiles in meibum obtained from other experimental animal models studied to date, e.g. rabbit.[5] It contains multiple ELCFA-based lipids, including surface-active lipids of the OAHFA family. Even the presence of a single mutated *Elovl4* allele, as in the Stgd3 mice in the current study, has functional consequences for anterior ocular surfaces. Phenotypic changes observed in heterozygous mice included increased blink rate, a preference for maintaining their eyes partially closed, and anatomical MG changes. Such changes are consistent with clinical findings in human patients with the evaporative form of DED, suggesting that further studies in ELOVL4 mutant mice offers a unique opportunity to investigate the role of specific lipids in meibomian gland and tear film biology and pathology.

Acknowledgments

Supported by National Institutes of Health Grant R01EY019480 (IAB), Vision Research Core Grant P30EY020799, and an unrestricted grant from Research to Prevent Blindness, Inc.

Disclosure: **A. McMahon**, None; **H. Lu**, None; **I.A. Butovich**, None

References

1. Meibom H. *De Vasis Palpebrarum Novis Epistolae Helmestadi: Typis & Sumptibus*. Helmstadt, Germany: Henningi Mulleri; 1666.
2. Knop E, Knop N, Millar T, Obata H, Sullivan DA. The international workshop on meibomian gland dysfunction: report of the subcommittee on anatomy, physiology, and pathophysiology of the meibomian gland. *Invest Ophthalmol Vis Sci*. 2011;52:1938–1978.
3. Butovich IA. Lipidomics of human meibomian gland secretions: chemistry, biophysics, and physiological role of meibomian lipids. *Prog Lipid Res*. 2011;50:278–301.
4. Butovich IA. Tear film lipids. *Exp Eye Res*. 2013;117:4–27.
5. Butovich IA, Lu H, McMahon A, Eule JC. Toward an animal model of the human tear film: biochemical comparison of the mouse, canine, rabbit, and human meibomian lipidomes. *Invest Ophthalmol Vis Sci*. 2012;53:6881–6896.
6. Nicolaides N, Kaitaranta JK, Rawdah TN, Macy JI, Boswell FM III, Smith RE. Meibomian gland studies: comparison of steer and human lipids. *Invest Ophthalmol Vis Sci*. 1981;20:522–536.
7. Butovich IA. The meibomian puzzle: combining pieces together. *Prog Retin Eye Res*. 2009;28:483–498.
8. Harvey DJ, Tiffany JM, Duerden JM, Pandher KS, Mengher LS. Identification by combined gas chromatography-mass spectrometry of constituent long-chain fatty acids and alcohols from the meibomian glands of the rat and a comparison with human meibomian lipids. *J Chromatogr*. 1987;414:253–263.
9. Tiffany JM. Individual variations in human meibomian lipid composition. *Exp Eye Res*. 1978;27:289–300.
10. Butovich IA, Wojtowicz JC, Molai M. Human tear film and meibum. Very long chain wax esters and (O-acyl)-omega-

hydroxy fatty acids of meibum. *J Lipid Res*. 2009;50:2471–2485.

11. Chen J, Green-Church KB, Nichols KK. Shotgun lipidomic analysis of human meibomian gland secretions with electrospray ionization tandem mass spectrometry. *Invest Ophthalmol Vis Sci*. 2010;51:6220–6231.
12. Lam SM, Tong L, Yong SS, et al. Meibum lipid composition in Asians with dry eye disease. *PLoS One*. 2011;6:e24339.
13. Green-Church KB, Butovich I, Willcox M, et al. The international workshop on meibomian gland dysfunction: report of the subcommittee on tear film lipids and lipid-protein interactions in health and disease. *Invest Ophthalmol Vis Sci*. 2011;52:1979–1993.
14. Butovich IA. Fatty acid composition of cholesteryl esters of human meibomian gland secretions. *Steroids*. 2010;75:726–733.
15. Agbaga MP, Brush RS, Mandal MN, Henry K, Elliott MH, Anderson RE. Role of Stargardt-3 macular dystrophy protein (ELOVL4) in the biosynthesis of very long chain fatty acids. *Proc Natl Acad Sci U S A*. 2008;105:12843–12848.
16. Ohno Y, Suto S, Yamanaka M, et al. ELOVL1 production of C_{24} acyl-CoAs is linked to C_{24} sphingolipid synthesis. *Proc Natl Acad Sci U S A*. 2010;107:18439–18444.
17. Yu M, Benham A, Logan S, et al. ELOVL4 protein preferentially elongates 20:5n3 to very long chain PUFAs over 20:4n6 and 22:6n3. *J Lipid Res*. 2012;53:494–504.
18. Bernstein PS, Tammur J, Singh N, et al. Diverse macular dystrophy phenotype caused by a novel complex mutation in the ELOVL4 gene. *Invest Ophthalmol Vis Sci*. 2001;42:3331–3336.
19. Edwards AO, Donoso LA, Ritter R III. A novel gene for autosomal dominant Stargardt-like macular dystrophy with homology to the SUR4 protein family. *Invest Ophthalmol Vis Sci*. 2001;42:2652–2663.
20. Maugeri A, Meire F, Hoyng CB, et al. A novel mutation in the ELOVL4 gene causes autosomal dominant Stargardt-like macular dystrophy. *Invest Ophthalmol Vis Sci*. 2004;45:4263–4267.
21. Zhang K, Kniazeva M, Han M, et al. A 5-bp deletion in ELOVL4 is associated with two related forms of autosomal dominant macular dystrophy. *Nat Genet*. 2001;27:89–93.
22. Li W, Chen Y, Cameron DJ, et al. Elovl4 haploinsufficiency does not induce early onset retinal degeneration in mice. *Vision Res*. 2007;47:714–722.
23. Raz-Prag D, Ayyagari R, Fariss RN, et al. Haploinsufficiency is not the key mechanism of pathogenesis in a heterozygous Elovl4 knockout mouse model of STGD3 disease. *Invest Ophthalmol Vis Sci*. 2006;47:3603–3611.
24. Cameron DJ, Tong Z, Yang Z, et al. Essential role of Elovl4 in very long chain fatty acid synthesis, skin permeability barrier function, and neonatal survival. *Int J Biol Sci*. 2007;3:111–119.
25. Vasireddy V, Uchida Y, Salem N Jr, et al. Loss of functional ELOVL4 depletes very long-chain fatty acids ($>$ or $=C_{28}$) and the unique omega-O-acylceramides in skin leading to neonatal death. *Hum Mol Genet*. 2007;16:471–482.
26. McMahon A, Butovich IA, Mata NL, et al. Retinal pathology and skin barrier defect in mice carrying a Stargardt disease-3 mutation in elongase of very long chain fatty acids-4. *Mol Vis*. 2007;13:258–272.
27. Karan G, Yang Z, Zhang K. Expression of wild type and mutant ELOVL4 in cell culture: subcellular localization and cell viability. *Mol Vis*. 2004;10:248–253.
28. Li W, Sandhoff R, Kono M, et al. Depletion of ceramides with very long chain fatty acids causes defective skin permeability barrier function, and neonatal lethality in ELOVL4 deficient mice. *Int J Biol Sci*. 2007;3:120–128.
29. McMahon A, Jackson SN, Woods AS, Kedzierski WA. Stargardt disease-3 mutation in the mouse Elovl4 gene causes retinal deficiency of C32-C_{36} acyl phosphatidylcholines. *FEBS Lett*. 2007;581:5459–5463.
30. Carson FL, Martin JH, Lynn JA. Formalin fixation for electron microscopy: a re-evaluation. *Am J Clin Pathol*. 1973;59:365–373.
31. Shelton JM, Lee MH, Richardson JA, Patel SB. Microsomal triglyceride transfer protein expression during mouse development. *J Lipid Res*. 2000;41:532–537.
32. Parakkal PF, Matoltsy AG. The fine structure of the lipid droplets in the meibomian gland of the mouse. *J Ultrastruct Res*. 1964;10:417–421.
33. Camera E, Ludovici M, Galante M, Sinagra JL, Picardo M. Comprehensive analysis of the major lipid classes in sebum by rapid resolution high-performance liquid chromatography and electrospray mass spectrometry. *J Lipid Res*. 2010;51:3377–3388.
34. Nicolaides N, Ansari MN, Fu HC, Lindsay DG. Lipid compsition on comedones compared with that of human skin surface in acne patients. *J Invest Dermatol*. 1970;54:487–495.
35. Westerberg R, Tvrdik P, Unden AB, et al. Role of ELOVL3 and fatty acid chain length in development of hair and skin function. *J Biol Chem*. 2004;279:5621–5629.
36. Butovich IA. On the presence and role of polar lipids in meibum. *Invest Ophthalmol Vis Sci*. 2010;51:6908–6910.
37. Butovich IA. Cholesteryl esters as a depot for very long chain fatty acids in human meibum. *J Lipid Res*. 2009;50:501–513.
38. Butovich IA, Arciniega JC, Lu H, Molai M. Evaluation and quantitation of intact wax esters of human meibum by gas-liquid chromatography-ion trap mass spectrometry. *Invest Ophthalmol Vis Sci*. 2012;53:3766–3781.
39. Guillou H, Zadravec D, Martin PG, Jacobsson A. The key roles of elongases and desaturases in mammalian fatty acid metabolism: Insights from transgenic mice. *Prog Lipid Res*. 2010;49:186–199.
40. Jakobsson A, Westerberg R, Jacobsson A. Fatty acid elongases in mammals: their regulation and roles in metabolism. *Prog Lipid Res*. 2006;45:237–249.
41. Mandal MN, Ambasudhan R, Wong PW, Gage PJ, Sieving PA, Ayyagari R. Characterization of mouse orthologue of ELOVL4: genomic organization and spatial and temporal expression. *Genomics*. 2004;83:626–635.
42. Schuett BS, Millar TJ. An investigation of the likely role of (O-acyl) omega-hydroxy fatty acids in meibomian lipid films using (O-oleyl) omega-hydroxy palmitic acid as a model. *Exp Eye Res*. 2013;115C:57–64.
43. Butovich IA, Lu H, McMahon A, et al. Biophysical and morphological evaluation of human normal and dry eye meibum using hot stage polarized light microscopy. *Invest Ophthalmol Vis Sci*. 2014;55:87–101.
44. Lu H, Wojtowicz JC, Butovich IA. Differential scanning calorimetric evaluation of human meibomian gland secretions and model lipid mixtures: transition temperatures and cooperativity of melting. *Chem Phys Lipids*. 2013;170-171:55–64.
45. Gasser K, Fuchs-Baumgartinger A, Tichy A, Nell B. Investigations on the conjunctival goblet cells and on the characteristics of glands associated with the eye in the guinea pig. *Vet Ophthalmol*. 2011;14:26–40.
46. Gipson IK, Argueso P. Role of mucins in the function of the corneal and conjunctival epithelia. *Int Rev Cytol*. 2003;231:1–49.
47. Floyd AM, Zhou X, Evans C, et al. Mucin deficiency causes functional and structural changes of the ocular surface. *PLoS One*. 2012;7:e50704.

Investigative Ophthalmology & Visual Science

48. Kunert KS, Tisdale AS, Gipson IK. Goblet cell numbers and epithelial proliferation in the conjunctiva of patients with dry eye syndrome treated with cyclosporine. *Arch Ophthalmol*. 2002;120:330–337.
49. Gipson IK, Spurr-Michaud SJ, Senchyna M, Ritter R III, Schaumberg D. Comparison of mucin levels at the ocular surface of postmenopausal women with and without a history of dry eye. *Cornea*. 2011;30:1346–1352.
50. Sirigu P, Shen RL, Pinto da Silva P. Human meibomian glands: the ultrastructure of acinar cells as viewed by thin section and freeze-fracture transmission electron microscopies. *Invest Ophthalmol Vis Sci*. 1992;33:2284–2292.
51. Gorgas K, Volkl A. Peroxisomes in sebaceous glands. IV. Aggregates of tubular peroxisomes in the mouse meibomian gland. *Histochem J*. 1984;16:1079–1098.
52. Schneider MR, Paus R. Sebocytes, multifaceted epithelial cells: lipid production and holocrine secretion. *Int J Biochem Cell Biol*. 2010;42:181–185.

Investigative Ophthalmology & Visual Science